UiT The Arctic University of Norway

Institute for medical biology, Faculty of Health Sciences

Metabolic, morphologic and translational alterations during differentiation of the H9c2 cardiomyoblast cell line

Cathrine Furuheim Bryn

Master's thesis in Medicine (MED-3950), June 2021

Preface

The main aim of this work was to make adjustments to the current protocol for culturing of the H9c2 cardiomyoblast cell line. The experiments laying the groundwork for this thesis was performed in July 2019 and February 2020.

The idea for this study developed during my research year at the institute for medical biology (IMB) at the faculty for health sciences at the University of Tromsø (UiT). I was admitted to the integrated research program for medical students spring 2018, and started doing research using a cell line called H9c2 as the research model. During these experiments, I met obstacles with the culturing of these cells which I felt there was no current solution for. Together with my supervisor and co-supervisor, I started with experiments to try to solve some of these issues and contribute to the existing knowledge about the cell line.

I would like to thank my supervisor Dr. Anne Hafstad for allowing me to develop my own research ideas, and help and guidance whenever needed. I want to thank my co-supervisor Trine Lund for technical support, support in conducting experiments and for always cheering up a day in the lab. Lastly, I want to thank Dr. Åsa Birgisdottir for sharing knowledge and insights on our field of research during the process of writing this thesis.

Cathrine Furuheim Bryn
Tromsø, June 2021

Contents

Preface 1
1 Abstract 3
2 Introduction 3
3 Materials & methods 7
3.1 Cell culturing 7
3.2 Differentiation of H9C2 cells 8
3.2.1 Comparing various differentiating protocols 8
3.2.2 Differentiation for 5, 10 and 15 days. 8
3.3 High-resolution respirometry 8
3.3.1 Citrate Synthase Assay 9
3.3.2 Protocol for permeabilized cells 9
3.3.3 Protocol for intact cells. 10
3.4 RNA isolation and cDNA synthesis 12
3.5 Real-time quantitative PCR (RT-qPCR) 12
3.6 Immunostaining of H9c2 cells 14
4 Statistics 14
5 Results 14
5.1 Assessment of differentiation 14
5.2 Differentiation for 5, 10 and 15 days 16
5.2.1 Gene expression at different time points 16
5.2.2 Immunostaining 17
5.2.3 Respirometry 19
6 Discussion 23
7 References 27
8 Appendix 29
8.1 Appendix 1: Chemicals 29

1 Abstract

Heart failure is a condition with increasing incidence, and remains a global pandemic. In vitro studies of molecular mechanisms aid in understanding the processes leading to and augmenting heart failure. The H9c2 cell line is an established model for the research of cardiac metabolism, toxicity studies and heart failure, mainly due to its origin from myocardial tissue. It possesses the ability to differentiate from an embryonic undifferentiated phenotype toward a cardiac muscular phenotype, induced by all-trans-retinoic acid (RA) and low serum concentrations in the culturing media. The alterations following differentiation increases its resemblance with adult cardiomyocytes with regard to morphology and metabolism. This study aims to further increase knowledge about the cell line's metabolic and morphologic characteristics after RA-treatment. We differentiated H9c2 cells for 5, 10 and 15 days and assessed the cells by respirometry, real-time qPCR and immunostaining. Our results are not conclusive, but still shows major remodeling during RA-induced maturing of the H9c2 cells. During RA-induced differentiation the cells appear larger and elongated, ordering themselves in a parallel fashion. Results from qPCR shows an early increase in expression of structural genes, while metabolic genes are upregulated later in the differentiation. Results from respirometry shows increased oxidative phosphorylation and increased spare capacity due to increased mitochondrial content.

2 Introduction

The incidence of heart failure (HF) is still rising, and is considered a global pandemic (1). Heart failure is a clinical syndrome and the terminal manifestation of a series of pathological processes leading to a non-functional, poorly contracting heart (2, 3). This means that the pathophysiology and etiology of HF is complex, and the knowledge about the underlying mechanisms that ultimately leads to a failing heart is still to be fully understood (3). The patient group is heterogeneous and frequently have comorbidities, which complicates the study of the condition (4). Cellular and molecular mechanisms are therefore commonly studied by the use of in vitro cell and animal models. In vitro models of the heart are difficult to establish, as the heart have one very characteristic feature – it is continuously contracting. Additionally, cardiomyocytes have low proliferative capacity, which makes them difficult to culture and sustain over a longer period of time (5). The H9c2 cell line has been established as an important in vitro model for studies on the failing heart as well as toxicity studies and metabolic studies (6). The H9c2 cell line was isolated and immortalized in the late 1970s

from the ventricular part of a BDIX rat heart in a 13 days old embryo (7, 8). Because of its similar responses to hypertrophy and cardiotoxic agents as in vivo cardiomyocytes, it has become an established model for cardiac research (9). The H9c2 cell line is beneficial in use as it is easy to stimulate and treat, cheaper than animal studies and this is a resilient cell line.

One characteristic of heart failure is metabolic remodeling, and the study of metabolism in heart failure models is important to get a better understanding of the condition (10). As opposed to a primary cardiomyocyte, the H9c2 cells are not contracting and their metabolism are therefore much lower. Additionally the H9c2 cells are glycolytic whereas cardiomyocytes primarily have an oxidative metabolism. The mainly glycolytic profile of the undifferentiated H9c2 might be explained by their fetal origin. The fetal environment is more hypoxic with higher levels of lactate and lower levels of fatty acids compared to the adult heart (11). However, the H9c2 cell line possesses the ability to differentiate toward a cardiac phenotype under the right conditions. During this differentiation, the metabolism shifts from mainly glycolytic to more oxidative metabolism (8, 12). Although the metabolism changes towards oxidative during differentiation of the H9c2 cells, it is difficult to compare this with the maturing of the myocard that happens during the first days of life. However, we know that there is an increase in mitochondrial mass and that the main consumption of oxygen in a cell is through generation of adenosine triphosphate (ATP) in oxidative phosphorylation in the mitochondria (6, 12). The maturing of the H9c2 cells by RA-induced differentiation also creates a more energy efficient cell with better coupling between the glycolytic and oxidative pathway (11). The adult heart can utilize any substrate available, but in the healthy heart, the main substrate used for oxidative phosphorylation is free fatty acids (11, 13). The adult cardiomyocyte both requires, but also have better access to, oxygen, glucose and free circulating fatty acids than the fetal cardiomyocytes (11). Whether the H9c2 cells have a preference towards glucose or fatty acid utilization is unknown remains elusive.

Because of the continuous mechanical work, the heart requires a high delivery of substrates to produce ATP. ATP can be produced both via glycolytic and oxidative pathways, and in the heart the oxidative metabolism dominates (14). In fact, 95 % of all produced ATP comes from oxidative phosphorylation in the complexes in the inner membrane of the mitochondria (14). As the generation of ATP is essential for contraction, the myocytes are flexible in substrate utilization depending on workload, feeding state and pathophysiological processes proceeding heart failure (13). The mitochondrion plays a crucial role in the homeostasis of the cells, and is central in both health and pathological processes. ATP-production in the mitochondria

happens through oxidative phosphorylation (OXPHOS) (13). This is a process where at least five large proteins embedded in the inner mitochondrial membrane, cooperate to yield ATP (Fig. 1). Complex I-IV participate in the electron transport chain (ETC), where oxygen is ultimately reduced to water at complex IV. Complex I, III and IV are transmembrane, and simultaneously with receiving electrons, they transfer protons across the inner mitochondrial membrane to the intermembrane space (IMS) between the two double lipid membranes that makes the mitochondrial wall. The transfer of protons to IMS, generates an electrochemical gradient across the membrane. The last complex in oxidative phosphorylation is complex V or the ATP-synthase. The ATP-synthase consists of two functioning units, F_0 and F_1, where F_0 is within the inner mitochondrial membrane and F_1 is in the matrix. F_1 consists of several subunits that forms a rotating ring around a stalk. The energy released when ATP-synthase transport protons back to the mitochondrial matrix, causes a conformational change in F_1, which in turn, enables binding of adenosine diphosphate (ADP) and simultaneously phosphorylation of ADP to ATP (15, 16).

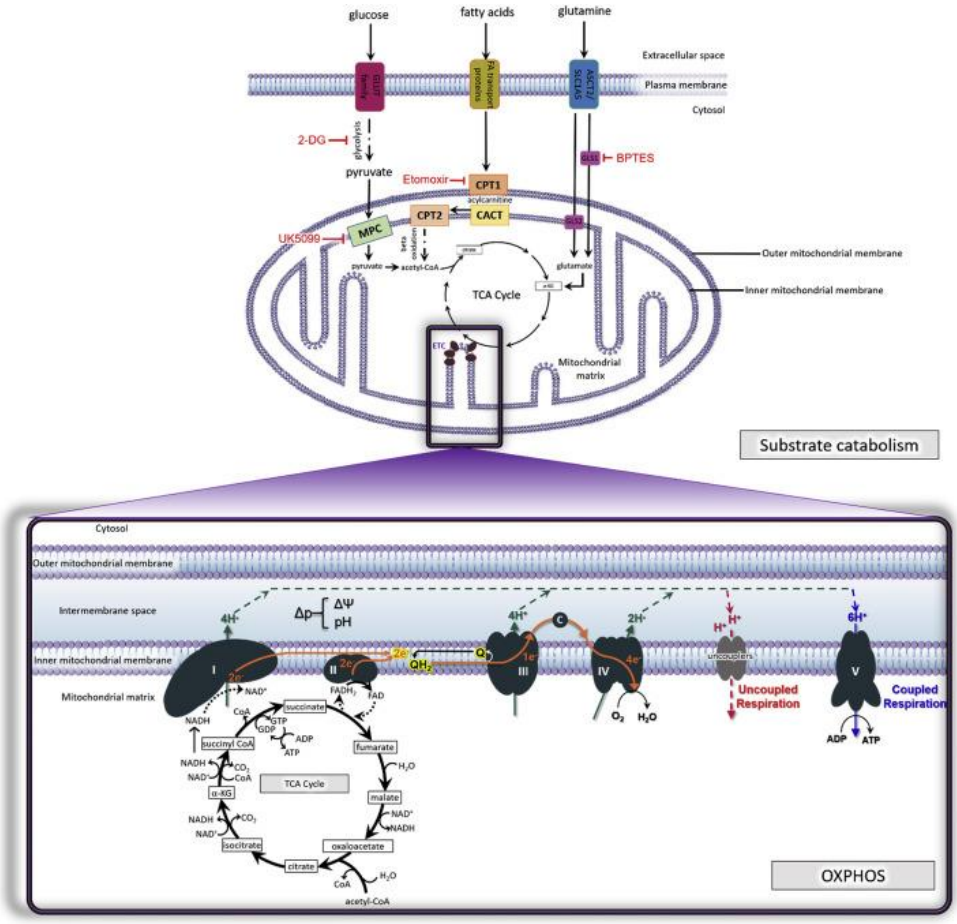

Figure 1: Schematic illustration of oxidative phosphorylation (OXPHOS) in the inner mitochondrial membrane. OXPHOS is closely linked to the tricarboxylic acid (TCA) cycle, as shown here, by feeding NADH and FADH2

to complex I and complex II respectively. OXPHOS include complex I-V, while natural uncouplers are important in case of high rate of substrate utilization and proton buildup in the inter membrane space (15).

The differentiation potential of the H9c2 cells is carried out by a protocol using all-trans-retinoic acid (RA) and lowering the concentration of fetal bovine serum (FBS) in the culturing media. RA-induced differentiation pushes the cells towards an adult cardiac phenotype. RA is a morphogen, known to be essential for the finely tuned embryonal development of the heart (17). Under culturing conditions with high levels of FBS, the cells have high proliferative capacity. By reducing the serum concentration, their proliferative capacity is lowered (18). The morphological changes are apparent after a few days of differentiation, where elongated cells are seen using a microscope. Simultaneously, the cells rearrange to order themselves in clusters in a parallel fashion. It is commonly claimed that during differentiation, the cells transform from mononucleated to multinucleated. If this happens by cell fusion or by a process of karyokinesis is somewhat unclear (19). Additionally, there has been shown presence of multinucleated cells at the undifferentiated state (5), while others have shown exclusively mononucleated cells in newly plated cells (19). Studies of genetic profiling of the RA-differentiated H9c2 cells are sparse, although some studies show that RA-induced maturation of the H9c2-cells have great impact on the gene expression and transcription. Cardiac specific markers like cardiac troponin T, myomesin2, myogenin, ryanodine receptor 1, sarcolipin and sarcoplasmic calcium transporter ATP2a1 has shown to be upregulated in several studies (6, 8, 20), and can be used to confirm the validity of the differentiation protocol. There has been shown an upregulation of genes involved in mitochondrial energy production, i.e. genes involved in oxidative phosphorylation as well as upregulation of genes involved in handling of fatty acids (8). There has also been shown an upregulation of the uncoupling proteins UCP2 and UCP3. Uncoupling proteins are located in the inner mitochondrial membrane, and are involved in the regulation of the proton gradient. This supports the knowledge that the mature H9c2 cell line is mainly oxidative, even though the high turnover of ATP for contraction is absent in a non-beating cell line.

Even, being a popular model for cardiac research, the H9c2 cell line has lost many of its cardiac properties, such as the morphology and the contracting phenotype of primary cells. This is apparent with the first glance in the microscope, and is due to lack of the classical organization of the contractile apparatus, which make up a great part of the cytoskeleton and thereby the shape and mechanical function of the cells. The characteristics of the differentiated cells are still to be fully understood, and more knowledge about the cell will

enable improved protocols for culturing of the cells. Although the protocol seems straight forward, there is no straight forward way to assure that the cells have reached a differentiated state, if they are to be used for other purposes (11). When assessing the cells in the microscope after 5 days, the morphological changes are obvious. However, it is also apparent that the population is not homogenous. The differentiation protocol used at our research group is a 5-day protocol using 1µM RA and 1% FBS in the culturing media. This is a well-established protocol, but there is no good evidence for the duration of the protocol, and there are little literature testing longer/shorter protocols. There has been suggested that other growth factors than RA could be used to induce differentiation towards a cardiac phenotype in the H9c2 cell line (21). Studies show that activation of the phosphoinositide-3 kinase (PI3K) and protein kinase C-δ (PKC- δ) pathways are involved in differentiation of cardiomyocytes and H9c2 cells (7). These pathways also have important roles both in physiologic and pathophysiologic hypertrophy. The binding of interleukin-6 (IL-6) to the IL-6 receptor activates PI3K and PKC-δ pathways, and thus makes IL-6 a contributor to cardiac hypertrophy (22, 23). There are few studies on the effect of IL-6 on the embryonic H9c2 cells, but one study shows that treating H9c2 cells with IL-6 induces differentiation(22).

The main aim for this work was to make adjustments to the existing protocol for differentiation of H9c2 cells in order to culture a more homogenous cell population of cells with a cardiac phenotype. Additionally, we wanted to do experiments with other growth factors to look for any synergistic effect. We have performed experiments using IL-6 for differentiation with or without RA and FBS. We wanted to investigate the effect of a longer differentiation protocol on gene expression, metabolism and the morphologic alterations and did experiments of differentiation for 5, 10 and 15 days

3 Materials & methods

3.1 Cell culturing

The H9c2 cells were cultured in Dulbecco's Modified Eagles medium (DMEM) with high glucose concentration of 4500 mg/L (HG DMEM), supplemented with 10% FBS (Sigma-Aldrich), and 1% penicillin/streptomycin (Sigma-Aldrich) in a CO_2 incubator (Nuair, Plymouth, USA) at 37°C and 5% CO_2 humidified air. At 70-80% confluence they were passaged.

3.2 Differentiation of H9C2 cells

3.2.1 Comparing various differentiating protocols

Cells were plated in 6-well plates. At a confluence of about 60%, differentiation was initiated. The cells were treated for five days with five differentiation protocols and one control group. To differentiate the cells we lowered the concentration of fetal bovine serum (FBS) from 10% under culturing conditions to 1-2% during differentiation. We utilized RA (Sigma-Aldrich) at a concentration of 1µM, and IL-6 (Sigma-Aldrich) at a concentration of 10µg/L. The differentiation protocols were as follows: 1% FBS, 1%FBS + 1µM RA, 1% FBS, 1µM RA + 10µg/L interleukin 6, 2% FBS, 2% FBS + 10µg/L IL-6. Differentiation medium were changed every second day in the dark as RA is sensitive to light. After 5 days, the cells were harvested for cDNA synthesis and analysis of mRNA expression.

3.2.2 Differentiation for 5, 10 and 15 days.

Based on the results from the various differentiation strategies, we chose the 1%FBS + 1µM RA protocol to assess longer differentiation protocols and compared them to undifferentiated cells (T_0) Cells were differentiated for 5 (T_5), 10 (T_{10}) and 15 days (T_{15}). Experiments were performed on passage 9, 11 and 13. At a confluence of 50-60%, differentiation were initiated. Differentiation medium were changed every second day in the dark. After the designated duration of differentiation, the cells were harvest for gene expression analysis (rt-PCR), respirometry, and immunostaining.

3.3 High-resolution respirometry

Mitochondrial respiration/respirometry studies were performed to assess oxygen consumption in the cells after the predetermined days of differentiation. Respirometry was performed at T_0, T_5, T_{10} and T_{15}. Immediately before mitochondrial respiration, the cells were detached from the bottom of the flask using 2 ml trypsin (Sigma-Aldrich), neutralized with high glucose (HG) DMEM, 10% FBS and transferred to a 15 ml Falcon tube. The cell suspension was centrifuged for 5 minutes at 500 G, and the supernatant was removed. The remaining cell pellet was then diluted in 0.8 ml respiration medium and the cell concentration was quantified using a Countess IIFL cell counter (Invitrogen ThermoFischer, Roskilde, Denmark). The cell concentration was used to calculate volume needed of the cell suspension to obtain 600 000 cells in each respiration chamber. Measurement of oxygen consumption in the cells were performed using a high-resolution respirometer (Oxygraph 2K, Oroboros Instruments, Innsbruck, Austria) and data recorded using the Datlab4 software (Oroboros instruments). On

each cell passage, we did respirometry both on intact and permeabilized cells. The data results from respirometry were normalized to «per million cells" obtained from the cell count and to citrate synthase (CS) activity.

3.3.1 Citrate Synthase Assay

Stored cells (-70°C) in MiR05 were analyzed for citrate synthase activity. Briefly this was done in the following manner. TritonX100, 4 µL of the cell sample was added to the assay buffer consisting of 0,25% 0.31 mM acetyl coenzyme A, 0,5 mM oxaloacetate (in 0.1M triethanolamine-HCl buffer, pH 8.0). The kinetic enzyme reaction was initiated by adding 0.1 mM 5,5′-Dithiobis(2- nitrobenzoic acid) (DTNB) dissolved in 1M Tris_HCl, pH 8,1. CS activity was determined by measuring optical density (OD) at 412 nm every 15 sec in 2-3 min using a microplate reader (VersaMax, Molecular Devices, San Jose, CA, USA). The CS activity is expressed as nmol/(mL*min). All chemicals were obtained from Sigma Aldrich.

3.3.2 Protocol for permeabilized cells

To permeabilize the cell membrane, we added 5µg/mL Digitonin, which allow added substrates to move freely from the media to the mitochondria. Permeabilized cells were respiring in Mir05 (Appendix 1) with no substrates initially, however addition of substrates are necessary to feed the oxidative phosphorylation. 5µM Carnitine, 1mM Malate, 10µM Palmitate and 5mM Pyruvate was added as substrates for oxidative phosphorylation through complex I and electron-transferring flavoprotein complex (CETF). 2.5mM ADP was then added as a substrate for ATP-synthesis. In order to assess whether the mitochondrial membrane was intact, we added 10µM Cytochrome C. 10mM Succinate was added as a substrate for complex II. Figure 2 shows a representative example of the protocol used, with sequential addition of chemicals.

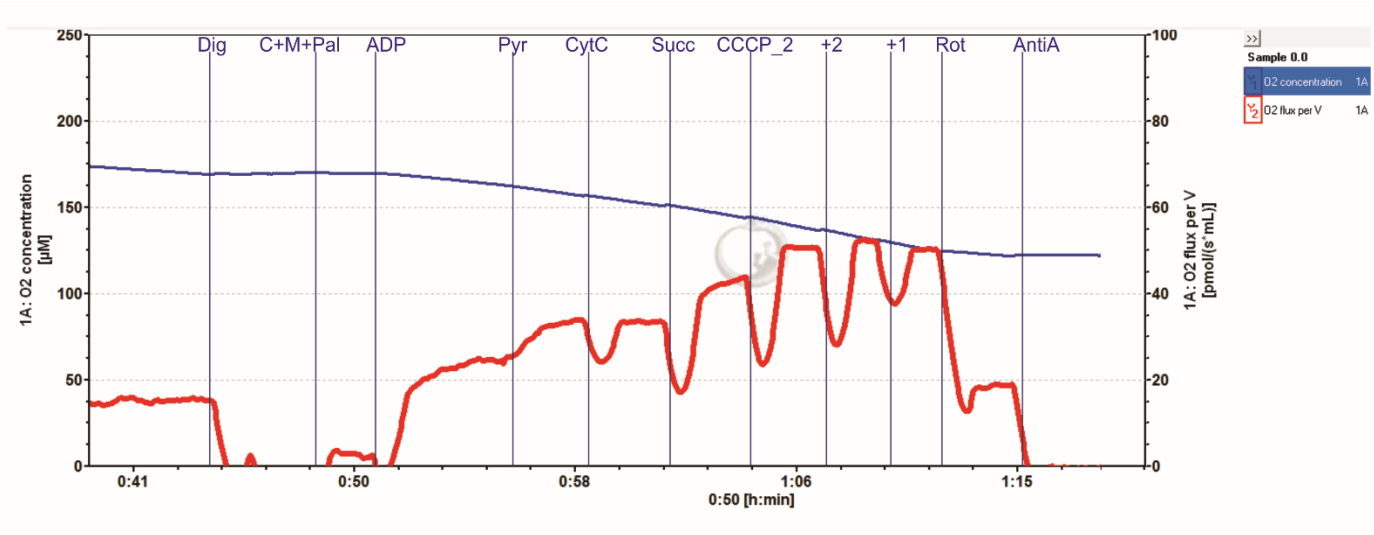

Figure 2: A representative example of the protocol for permeabilizing the cells. The permeabilized protocol uses Mir05 as respiration medium. Substrates to feed oxidative phosphorylation, is added during the experiment. The chemicals are added to the chamber in the following order 1)Digitonin (Dig): To permeabilize the outer cellular membrane, and make the cell available for substrates. 2) Carnitine, Malate & Palmitate (C+M+Pal): Substrates for complex I in oxidative phosphorylation. 3) Adenosine diphosphate (ADP): Added as a substrate for ATP synthesis at complex V (ATP synthase). 4) Pyruvate (Pyr): Is added as a substrate for complex I. 5) Cytochrome C (CytC): Added to assess the outer mitochondrial membrane. 6) Succinate (Succ): Added as a substrate for complex II. 7) Carbonyl cyanide m-chlorophenylhydrazone (Cccp): Added by titration, indicated with 2+ mark in the figure, until maximal oxygen consumption is reached. Cccp is a protonophore enabling protons to leak across the inner mitochondrial, and free-couple electron transport chain from ATP-synthesis at complex V. 8) Rotenone (Rot): Rotenone is added to inhibit respiration through complex I. 9) AntimycinA (AntiA): Added to inhibit complex III and measure oxygen consumption through complex I and III.

3.3.3 Protocol for intact cells.

Intact cells were respiring in HG DMEM supplemented with 20 µM palmitate, 1mM pyruvate and 5mM HEPES. Sequential addition of complex inhibitors influences the oxygen consumption rates as shown in figure 3. 10nM oligomycin, an inhibitor of ATP-synthase, was added to measure proton leak caused by the proton gradient across the inner mitochondrial membrane. 0.4-0.9µM Carbonyl cyanide m-chlorophenyl hydrazine (Cccp) was added by titration to free-couple the electron transfer (use of oxygen) from the phosphorylation of ADP to ATP. This enables measurement of the cells' maximal capacity to reduce oxygen and respire under the experimental conditions. Adding 0.5µM rotenone inhibits complex I, and 2.5µM Antimycin A inhibits the cytochrome C reductase (complex III).

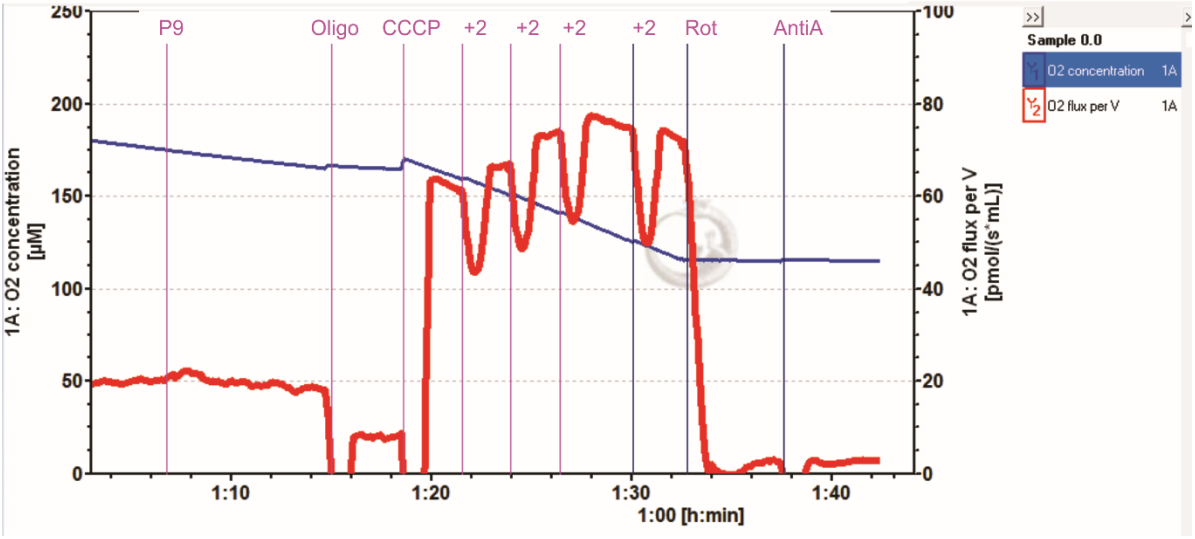

*Figure 3: A representative example of the protocol for intact cells. Red line: O_2 flux per volume (pmol/s^{-1}*ml). Blue line: Oxygen (µM) concentration in the chamber. X-axis: time (h:min). Vertical lines marks addition of a chemical to the respiration chambers. The protocol for additions of chemicals is as follows:1) Oligomycin (Oligo): Inhibitor of the ATP-Synthase. 2) Carbonyl cyanide m-chlorophenylhydrazone (Cccp): Free-couples the electron transport chain from the phosphorylation at complex V (ATP-Synthase). Cccp is added by titration until a maximum oxygen consumption is reached (indicated in the figure with the +2 mark). 3) Rotenone (Rot): Inhibitor of complex I. 4) Antimycin A (AntiA): Inhibitor of complex III.*

The inhibitors and free-coupler (Cccp) used in the protocol for intact cells (Fig. 4) can be used to further examine several parameters and characteristics of the cells, as shown in figure 3.

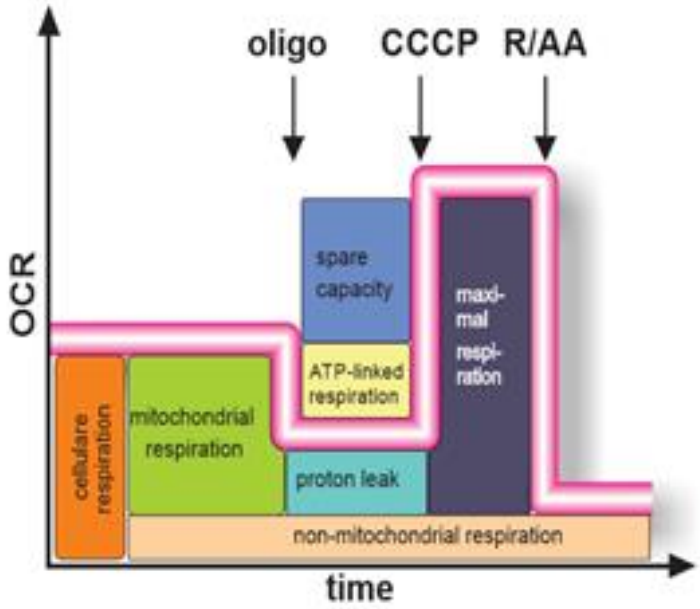

Figure 4: The cellular bioenergetic profile. Parameters we can assess using the protocol for intact cells. The figure is adapted from the work of Chacko et. Al (2014). Analysis of the bioenergetic profile for a cell can be

used to measure several indicators of mitochondrial respiration in intact cells in real-time. It may identify respiratory changes and defects. First in the protocol, cellular respiration (orange box in the illustration) is recorded and represent all the processes consuming oxygen in the cells, under the context given by the media composition. This include both mitochondrial respiration and other oxidases. Next, oligomycin an inhibitor of ATP-Synthase is added, and respiration linked to ATP production is uncovered (yellow box). Furthermore, Cccp a proton ionophore is titrated step-wice to generate the maximal respiration. Then the electron transfer is not anymore controlled by the proton gradient and ATP-Synthase activity. This is mirroring the spare capacity for the mitochondria (light blue box). Non-mitochondrial O_2 use consumption by the cell is emerging by using rotenone (CI inhibitor) and Antimycin A (CIII inhibitor). Finally, the difference between oxygen consumption rate (OCR) with oligomycin and non-mitochondrial- mitochondrial O_2 consumption, reflects the proton-leak (green box). For review, see Chacko with coworkers 2014 and Hill with coworkers 2012.(24, 25).

3.4 RNA isolation and cDNA synthesis

Cells intended for RNA-isolation were cultured in 6-well plates. Examining altered gene expression is performed in a three-step manner, where the first step is to isolate RNA from the cells. The total RNA was isolated from the H9c2 cells according to the protocol for the RNaeasy Plus Mini kit (Qiagen, Hilden, Germany).

Step two is to synthesize cDNA from the isolated RNA. cDNA synthesis was performed using the High Capacity cDNA Reverse Transcription kit (Applied Biosystems) according to the manufacturer's protocol.

3.5 Real-time quantitative PCR (RT-qPCR)

The third step in examining gene expression is analysis of the cDNA using polymerase chain reaction (PCR). Primers (table 1) used in the qPCR were obtained from Sigma, and for each run we used Fast Start Essential DNA Green Master (Roche diagnostics, Mannheim, Germany). The real-time PCR reactions were analyzed in Roche LightCycler96 (Roche diagnostics) with 40 PCR cycles and melting curve analysis after the PCR. Quantification cycle (Cq) is automatically reported by the Light cycle software 4.1. Cq 37 was set as the highest Cq that was possible to accurate measure. Analyzed genes were chosen, based on existing literature and our own previous research.

The expression of genes is normalized to a reference gene. We tested four different reference genes, and chose the most stable gene according to the results from the GeNorm-analyzis (26). mRNA expression was also normalized to the control group, i.e. the undifferentiated cells. In the differentiation protocols using IL-6, *cyclo* was set as reference gene. In the differentiation protocols of varying duration, *gapdh* was set as reference gene.

Table 1: Forward and reverse primers used in qPCR with primer sequences.

Gene	Protein	Function	Sequence
Tnnt2	Cardiac Troponin T	Structural/Differentiation	FP: CGACCACCTGAATGAAGACC RP: CGGCCTCTAGGTTGTGGA
Myom2	Myomesin2	Differentiation	FP: AATCGTGGCAAGGTGATTG RP: GTGCAGGTGAGGTTCAAGGT
ATP2a2	ATPase, Ca++ transporting, cardiac muscle, slow twitch 2 (Serca2)	Calciumhandling/Differentiation	FP: GAGAACGCTCACACAAAGACC RP: CAATTCGTTGGAGCCCCAT
PGC1β	Peroxisome profliferator-activated receptor gamma, coactivator 1 beta	Metabolic	FP: TGGCCCAGATACACCGACTA RP: TTGCTTTTCCCAGACGAGGG
SLC25A4	Adenine nucleotide translocase (ANT1)	Metabolic	FP: CCTCTGCTTCGTCTACCCAC RP: GACCCTTCAGGCCATCAGAC
UCP3	Uncoupling protein 3	Metabolic	FP: TACAGAACCATCGCCAGGA RP: TATCGGGTCTTTACCACATCCA
PDK4	Pyruvate dehyodreganse Kinase 4	Metabolic	FP: GCATTTCTACTCGGATGCTCATG RP: CCAATGTGGCTTGGGTTTCC
CD36	CD36	Metabolic	FP: GCGACATGATTAATGGCACA RP: TGGACCTGCAAATGTCAGAG
CPT1α	Carnitine Palmitoyltransferase 1A	Metabolic	FP: GCACCAAGATCTGGATGGCTTATGG RP: TACCTGCTCACAGTATCTTTGAC
Plin2	Perilipin2	Metabolic	FP: AGAAGGAGCTCGAGAAAGCAA RP:TTGTTTGGCGTCTTTGATCCTGCC
GAPDH	Glyceraldehyde 3-phosphate dehydrogenase	Housekeeping gene	FP: TGGGAAGCTGGTCATCAAC RP: GCATCACCCCATTTGATGTT
CYCLO	Peptidylprolyl isomerase A	Housekeeping gene	FP: CTGATGGCGAGCCCTTG RP: TCTGCTGTCTTTGGAACTTTGTC

3.6 Immunostaining of H9c2 cells

Undifferentiated cells and differentiated cells (T_0, T_5, T_{10} and T_{15}) were seeded on glass coverslips and fixed (4% PFA for 20 min at 37 °C). Before immunostaining, cells were permeabilized with methanol for 5 min. The permeabilized cells were blocked with 3% goat serum in PBS for 1 hour, before incubation with the primary antibody (anti-TOM20 FL-145 1:500 dilution) and incubated overnight (4 °C). Cells were washed 6 x in PBS and incubated with the secondary antibody (Alexa 488 anti-rabbit antibody, Invitrogen,1:500 dilution) and PE conjugated cardiac troponin T antibody (Miltenyi Biotek, 1:50 dilution) in 1% goat serum for 1 hour in room temperature. Before mounting, cells were washed and stained with DAPI (1:1000, 5 min). Confocal images were obtained using a 40x/NA1.2 water immersion objective on a LSM780 (Carl Zeiss) using the ZEN Imaging Software.

4 Statistics

The results are presented as means ± standard error of means (SEM) in column bar graphs. In order to compare differences between two groups, paired Student's t-tests were performed.

5 Results

5.1 Assessment of differentiation

In order to investigate the differentiation protocols for H9c2 cells further, we initially treated undifferentiated H9c2 cells for five days using different protocols. We did qPCR on selective genes related to differentiation and metabolism.

The protocol using 1% FBS for differentiation has 6.7-fold upregulation of myomesin-2 (*myom2*) (Fig. 5). Myomesin2 also called M-protein is part of the myomesin family, proteins that constitute the M-band and present in the adult heart and fast fibers (27, 28). There is also a 3.6-fold increase in mRNA expression of cardiac Troponin T (*tnnt2*). These results indicate a differentiation towards a muscular phenotype. Differentiation using 1% FBS with RA shows the same trend as with 1% FBS, although with a higher increase in expression of *myom2* and *tnnt2* of 10.6 and 6.10-fold up. There is also an increase in mRNA expression of the gene coding for ATPase Ca^{2+} dependent slow-twitch cardiac muscle-2 protein (*atp2a2*), with a 1.9-fold increase. The peroxisome proliferator-activated receptor gamma coactivator 1 beta (*pgc1β*), encoding a protein involved in β-oxidation in the mitochondria and mitochondrial biogenesis (29) is 2.0-fold up. This gene increases its expression in the protocol with RA

compared to differentiation only using 1% FBS. Comparing to the control group, *pgc1β* has higher expression in the group treated with 1%FBS and RA (Fig. 4). In the group using 1% FBS, RA and IL-6 for differentiation, there is an increase in the expression of all of the tested genes compared to the control group. However, when comparing to the protocol only using 1% FBS and RA, the increase in *myom2*, *tnnt2* and *pgc1β*, is lower in the group adding IL-6 to the protocol. From these results, there is no apparent synergistic effect of adding IL-6 to the differentiation protocol when looking at these differentiation-related genes. The protocol using 2% FBS (Fig. 4) also increases its expression of *myom2* (3.8-fold up), *atp2a2* (1.25-fold up) and *tnnt2* (2.5-fold up) compared to the control group, but not when comparing to the group using 1% FBS in mono treatment. There are no significant alterations in the mRNA expression of *ant1* in either of these differentiation protocols.

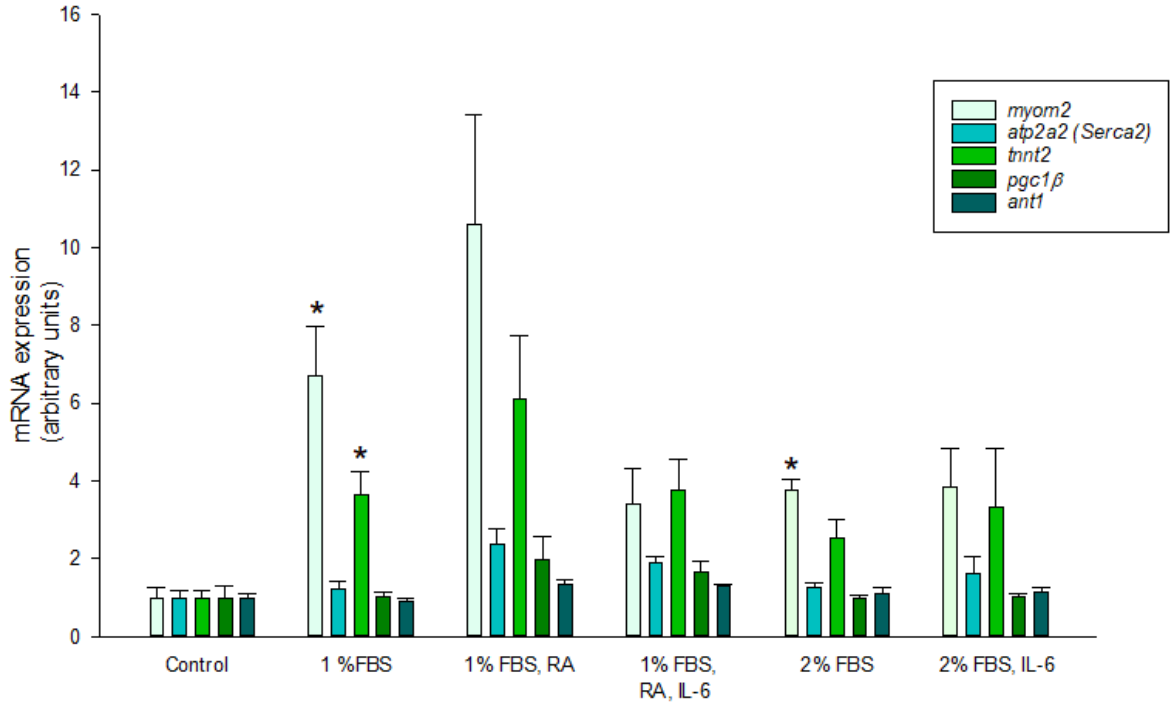

*Figure 2: mRNA expression of selected genes: Cardiac Troponin T (*tnnt2*), myomesin2 (myom2), ATPase Ca^{2+} dependent slow-twitch cardiac muscle-2 protein (*atp2a2*) peroxisome proliferator-activated receptor gamma coactivator 1 beta (*pgc1β*) and adenine nucleotide translocase type 1 (ant1) related to differentiation and metabolism in five different differentiation protocols. Control: Undifferentiated cells cultured in 10% FBS (fetal bovine serum). RA: All-trans retinoic acid. IL-6: Interleukin 6. Data are means ± SEM, n=4 in each group, *p<0.05 vs control.*

5.2 Differentiation for 5, 10 and 15 days

5.2.1 Gene expression at different time points

We have performed qPCR on selected structural and metabolic genes after differentiating the cells 0, 5, 10 or 15 days.

In the graph (Fig. 6), the expression of each gene is relative to level of expression in the undifferentiated cells. The expression of *atp2a2*, encoding sarcoplasmic reticulum calcium ATPase2 (SERCA2) had no significant change in expression at any time points (Fig. 6A). The expression of *tnnt2*, had a 13.8-fold increase at T_5 and a 12.2-fold increase at T_{10} and 6.0-fold increase at T_{15} (Fig. 5A). The expression of *myom2* was upregulated at T_5 with an 18.9-fold increase and further 32.9-fold increase at T_{10} compared to T_0. At T_{15} it is 25.8-fold up compared to T_0 (Fig. 6A). The expression of *pgc1β*, involved in mitochondrial biogenesis, is upregulated at T_5 with a 2.7-fold increase. At T_{10} and T_{15} it is 2.65 and 1.72 up respectively (Fig. 6B). C*d36*, coding for CD36 molecule and involved in fatty acid handling, has increased expression in all protocols compared to T_0 (Fig. 6C), although not statistically significant. U*cp3*, encoding uncoupling protein 3, is not expressed at T_0, but is upregulated at T_5 with a 76–fold increase and again at T_{10} with a 220-fold increase, with no further increase at T_{15} from T_{10} (Fig. 6D). P*dk4*, a mitochondrial related protein, is significantly upregulated at T_5 with a 76,8 fold increase, 994 fold up at T_{10} and 4355 fold up at T_{15} (Fig. 6E).

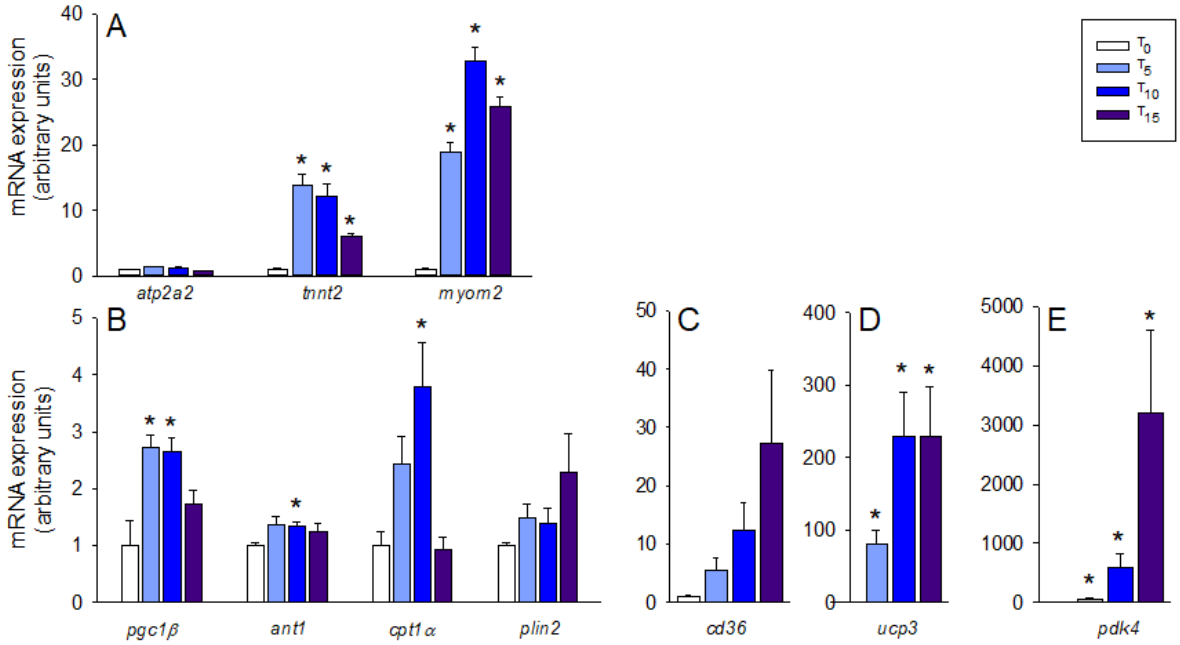

Figure 3: mRNA expression at T_0, T_5, T_{10} and T_{15} for selected genes. Data are means ± SEM, *n=4 in each group, *p<0.05 vs control.*

5.2.2 Immunostaining

During differentiation, the H9c2 cells changed morphology as illustrated in figure 7 showing representative pictures of immuno-stained cells from the different timepoints. H9c2 cells hypertrophied with differentiation together with elongation of the cells, compared to cells at T_0. Although not quantified in this study, the cell population appear more heterogeneous at T_5, T_{10} and T_{15} compared to what is seen at T_0. Staining of the mitochondrial outer membrane protein; TOM20 staining showed a more extensive network of mitochondria following differentiation, especially at T10 and T15, while the intensity of cardiac troponin T-stained cells seemed to peak around T_{10}.

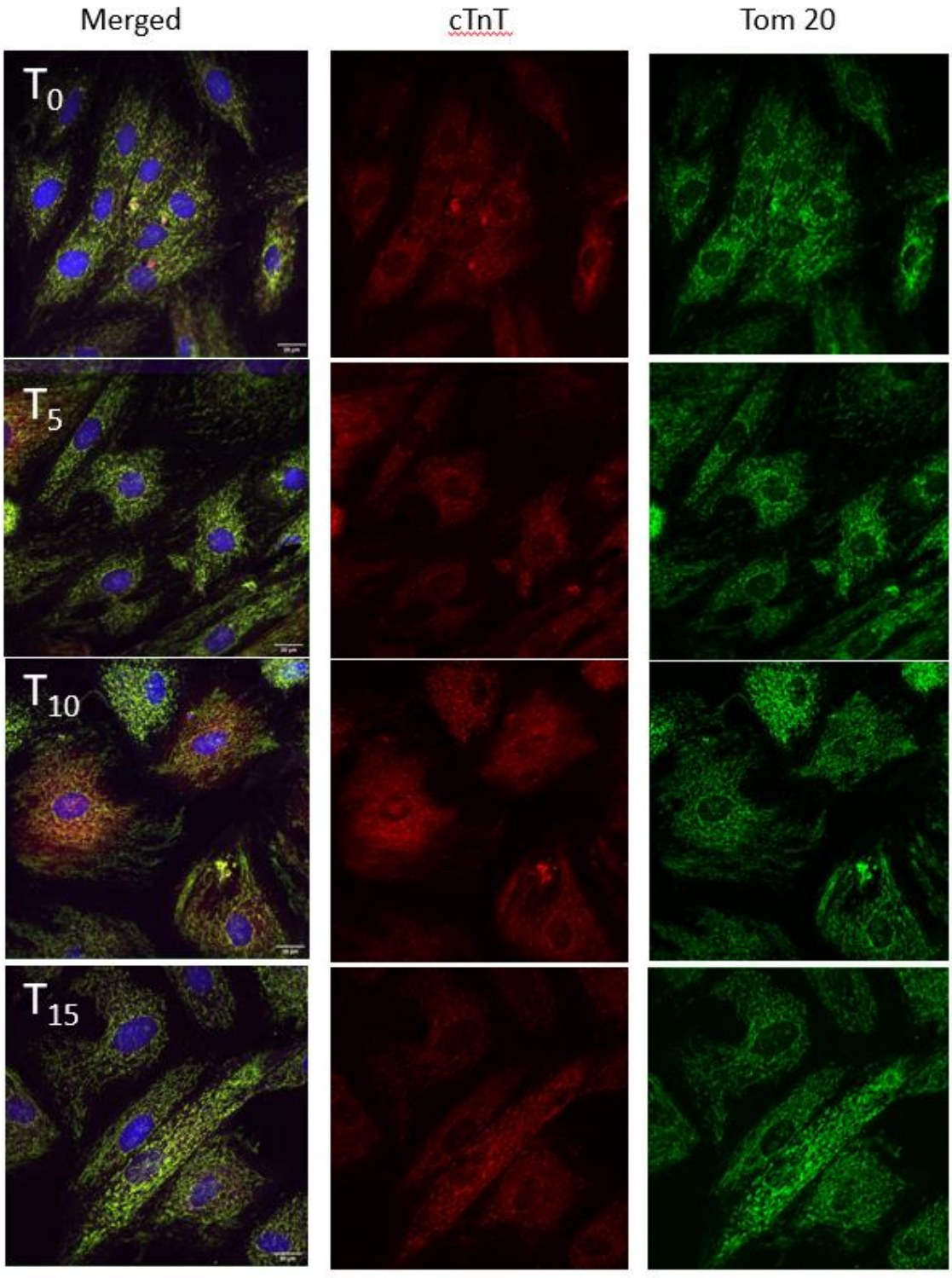

Figure 4: Representative pictures using confocal microscopy of differentiated H9c2 cells at different timepoints; 0, 5, 10 and 15 days (T_0, T_5, T_{10} and T_{15}). Cells were stained for cardiac troponin T (cTnT), mitochondrial network (Tom 20) and nucleus staining (DAPI). Scale bar is 20 µm.

5.2.3 Respirometry

5.2.3.1 Mitochondrial respiration with permeabilized cells

In order to further assess metabolic changes in the differentiated cells, we performed mitochondrial respiration.

Basal respiration (Fig. 8A) is not different between groups, although there is a trend for increased uncoupling using palmitate and carnitine as a substrate ($LEAK_{Pal}$) with increased length of the differentiation protocol (Fig. 8B). Similarly, there is also a trend for a steady increase in oxidative phosphorylation (OXPHOS) using these substrates ($OXPHOS_{Pal}$) with longer duration of differentiation (Fig. 8C). Adding pyruvate as a substrate for complex I (CI) induced a significant increase in $OXPHOS_{Pal+CI}$ versus undifferentiated cells, but only at T_{10} (Fig. 8D). Adding succinate as a complex II (CII) substrate did not result in a substantial increase in OXPHOS ($OXPHOS_{Pal + CI + CII}$, Fig. 8G). Due to the selected protocol, it is not possible to distinguish the CII activity alone as succinate is added after the palmitate, carnitine and pyruvate. The electron transport chain (ETC) capacity in the mitochondria was measured following addition of Cccp, which free-couples the ETC from the phosphorylation. Again, ETC capacity was significantly increased at T_{10}, with a trend for increased ETC capacity at T_5 and T_{15} versus T_0 (Fig. 8G). We see the same trends for ETC-CI (Fig. 8H) when CI was inhibited by rotenone. Adding 10µM Cytochrome C (CytC) did not increase the OXPHOS respiration, indicating intact outer mitochondrial membrane in the cells, which was not affected by the differentiation protocols nor pre-experimental preparations (Fig. 8E).

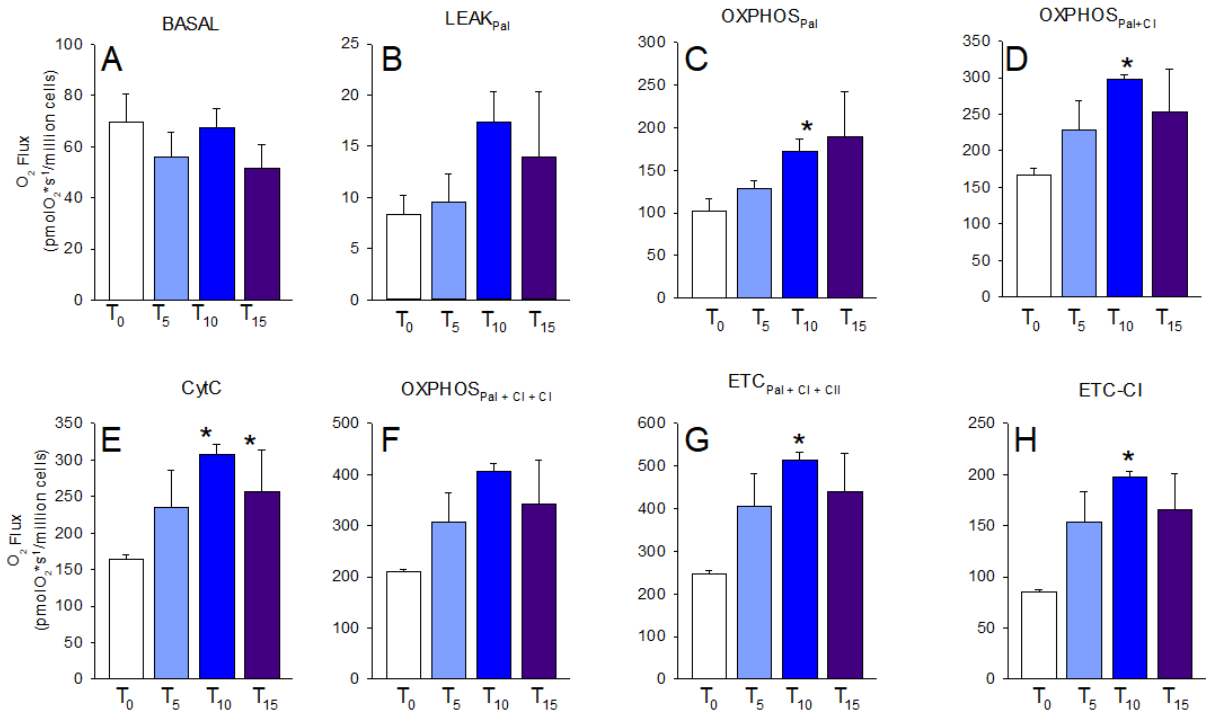

*Figure 8: A-H: Mitochondrial respiration measured in H9c2 cells permeabilized with 20 µg/ml digitonin and normalized to "per million cells". A (BASAL): Basal respiration prior to addition of substrates. B (LEAK$_{Pal}$): Leak-state measuring intrinsic uncoupling in the mitochondrial membrane after addition of complex I substrates (5µM carnitine, 1mM malate, 10µM palmitate). C (OXPHOS$_{Pal}$): Measuring oxidative phosphorylation through complex I and electron-transferring flavoprotein complex (CETF) after addition of 2.5mM ADP for ATP-synthesis. D (OXPHOS$_{Pal+CI}$):Measuring oxidative phosphorylation after 5mM pyruvate as a substrate complex I. E (CytC): 10µM Cytochrome C (Cytc) is added to assess whether the outer mitochondrial membrane is intact. F (OXPHOS$_{Pal+CI+CII}$): Measuring oxidative phosphorylation after addition of 10mM succinate as substrate for complex II. G (ETC$_{Pal+CI+CII}$): Oxygen consumption after addition of Carbonyl Cyanide m-Chlorophenyl hydrazine (Cccp) to free-couple the electron transport from complex I to complex IV from the phosphorylation at complex V and measuring the maximal electron transport capacity. H (ETC-CI): Measuring respiration after inhibiting complex I with 0.5µM rotenone. Values are mean ± SEM, n=3 in each group, *=p<0.05.*

When normalizing mitochondrial respiration to citrate synthase (CS) activity (Figure 9A-H), there is a significant reduced basal respiration at all subsequent time points (Fig. 9A). Interestingly, none of the other measured states were significantly altered by the differentiation protocols when the data were normalized to CS activity.

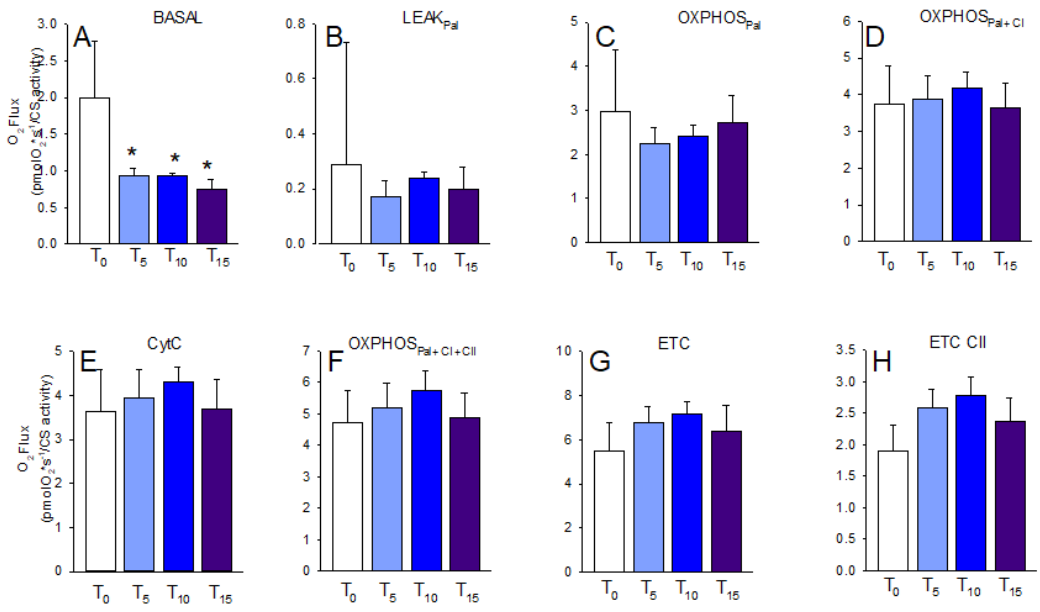

*Figure 9: A-H: Mitochondrial respiration measured in H9c2 cells permeabilized with 20 µg/ml digitonin and normalized to citrate synthase (CS) activity. A (BASAL): Basal respiration prior to addition of substrates. B (LEAK$_{Pal}$): Leak-state measuring intrinsic uncoupling in the mitochondrial membrane after addition of complex I substrates (5µM carnitine, 1mM malate, 10µM palmitate). C (OXPHOS$_{Pal}$): Measuring oxidative phosphorylation through complex I and electron-transferring flavoprotein complex (CETF) after addition of 2.5mM ADP for ATP-synthesis. D (OXPHOS$_{Pal+CI}$):Measuring oxidative phosphorylation after 5mM pyruvate as a substrate complex I. E (CytC): 10µM Cytochrome C (Cytc) is added to assess whether the outer mitochondrial membrane is intact. F (OXPHOS$_{Pal+CI+CII}$): Measuring oxidative phosphorylation after addition of 10mM succinate as substrate for complex II. G (ETC$_{Pal+CI+CII}$): Oxygen consumption after addition of carbonyl cyanide m-chlorophenyl hydrazine (cccp) to free-couple the electron transport from complex I to complex IV from the phosphorylation at complex V and measuring the maximal electron transport capacity. H (ETC-CI): Measuring respiration after inhibiting complex I with 0.5µM rotenone. Values are mean ± SEM, n=3, *=p<0.05.*

RA-induced differentiation is expected to increase the mitochondrial content in the H9c2 cells. One way to assess this, is through activity of the mitochondrial enzyme citrate synthase. Figure 10A shows that there is steady increase of CS-activity per protein with longer differentiation protocols. Figure 10B shows the correlation between cell count and protein concentration. There seems to be a linear correlation, although somewhat unclear probably due to few experiments.

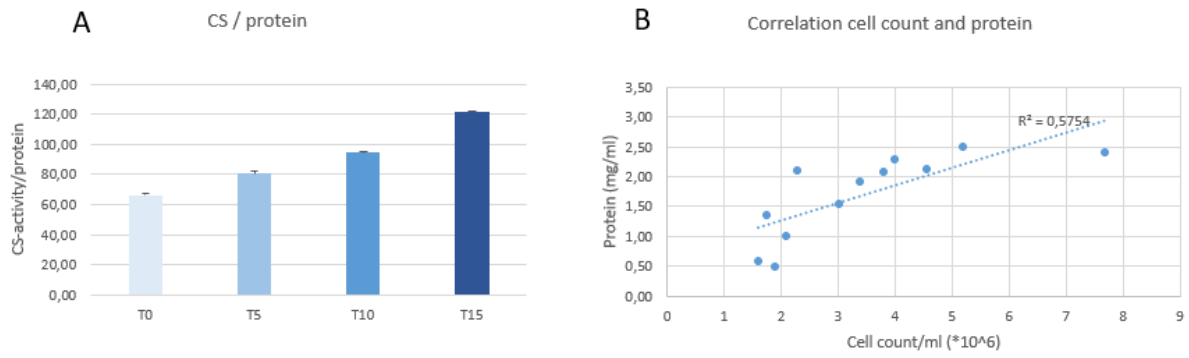

*Figure 10: A: Activity of the mitochondrial protein citrate synthase (CS) per protein concentration at T_0, T_5, T_{10} and T_{15}. CS-activity: nmol/ml*min. Protein-concentration: mg/ml. B: Correlation between measured protein concentration in the cell suspension and cell count in from the cell suspension. Cell count from the cell suspension were performed immediately before adding cells to the chamber at every experiment with mitochondrial respiration.*

5.2.3.2 Mitochondrial respiration with intact cells

There is a significant reduction in the basal respiration (Fig. 11A) from T_0 to T_5 and T_{10}. The basal respiration is overall higher in the intact cells, than the permeabilized, indicating affected respiration by the medium in which the cells respire during experiment. By adding oligomycin and inhibiting the ATP-Synthase, we can measure the natural uncoupling (Fig. 11B) or the LEAK. The oxygen consumption is significantly reduced from T_0 to the following time points in the differentiation protocol. The ETC (Fig. 11C) shows a trend of increased electron transport capacity with longer differentiation protocol. By adding rotenone, and inhibiting CI, there is a significant reduction in respiration from T_0 to the following time points in the protocol (Fig. 11D). The same trend was seen after addition of AntimycinA, inhibiting complex III (data not shown).

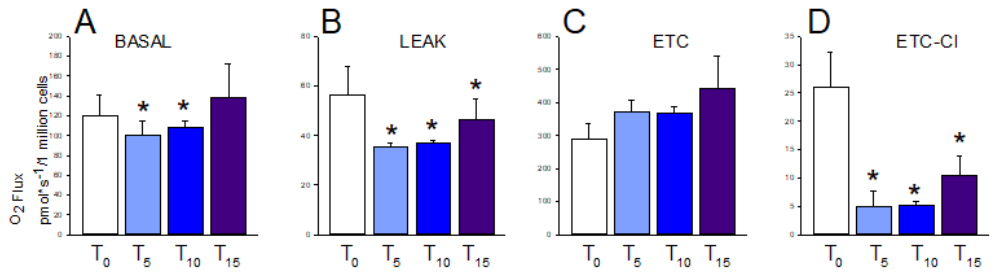

Figure 11: Mitochondrial respiration with intact cells, normalized to per million cells. A (BASAL): Basal respiration. Respiration measured before addition of any inhibitors. B (LEAK): Leak-state. Measuring leak of protons, not coupled to the respiratory complexes. C (ETC): Electron transport capacity (ETC) measures the maximal respiratory capacity of the cells by free-coupling protons from the electron transport chain. D (ETC-

*CI): Measures respiration after inhibiting complex I with rotenone, and therefore shows respiration through complex II, complex IV and non-mitochondrial respiration T_0: Undifferentiated. T_5: 5-day differentiation protocol. T_{10}: 10-day differentiation protocol. T_{15}: 15-day differentiation protocol. Values are mean ± SEM, n=3, *=p<0.05.*

When normalizing to CS-activity in intact cells, we saw the same trends as when normalizing to per million cells (data not shown).

Looking closer at the internal characteristic of the mitochondria, we normalized the data from respiration in each group to the measured maximal respiratory capacity (the ETC). By using the theory of mitochondrial bioenergetics from figure 3, we created sector diagrams for the each of the timepoints (Fig. 12, A-D). The diagrams show that there is a 14-10% increase in spare capacity with longer duration of the differentiation protocol. There is a 5-4% reduction in the LEAK from T_0 to the next time points. The ATP-linked respiration is reduced with longer differentiation protocol, and the same accounts for the non-mitochondrial respiration.

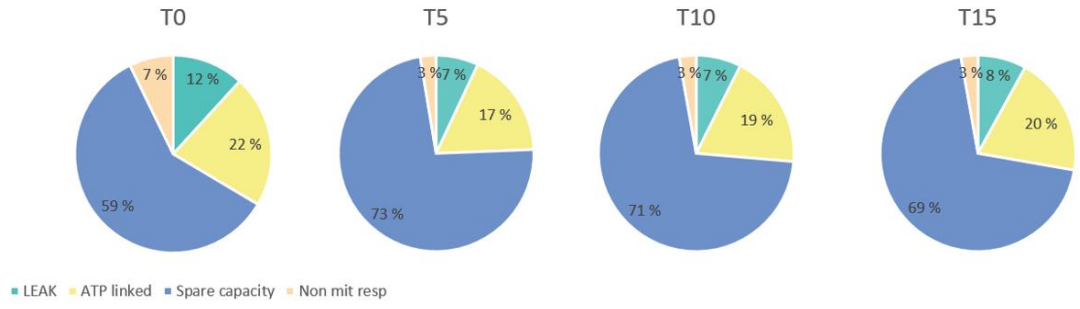

Figure 12: Respiratory data from intact cells relative to maximal respiratory capacity. Blue sector: Spare capacity of the cells. Yellow sector: ATP-linked respiration. Green sector: Proton leak across the mitochondrial membrane. Orange sector: Non-mitochondrial respiration.

6 Discussion

In the experiments comparing five separate differentiation protocols, we used the mRNA expression of *tnnt2* and *myom2*, which are related to differentiation in order to compare and select a differentiation protocol for the H9c2 cells. The use of different morphogens, other that RA (21) has been suggested, and one study have reported IL-6 to have the potential to differentiate H9c2 cells (22) we adopted the same protocol in the current study to compare it with the established protocol using RA. However, we were not able to reproduce the same results in our experiments as 2% FBS alone seemed to have the same potential for increasing markers of differentiation (*myom2* and *tnnt2*) as 2% FBS supplemented with IL-6. Even

though we were not able to reproduce the same results, IL-6 could be relevant to use in differentiation protocols, as it is known to activate pathways involved in differentiation and hypertrophy (7, 22, 30). Most research on the effect of IL-6 signaling is however performed on adult cardiomyocytes, while the undifferentiated H9c2 resembles an embryonic cardiomyoblast (22). In our hands the expression targeted differentiation genes (*myom2* and *tnnt2*) showed the highest increase in the protocol using RA and 1% FBS compared to the other differentiation protocols. From these results, we decided to use this protocol further for further differentiation.

Looking at various lengths of the RA and 1% FBS protocol, there is a transient upregulation of expression of *tnnt2* which peaks at T_5 and then has somewhat lower expressions in the next time points (T_{10} and T_{15}) as compared to T_5. Because we see morphological changes early in the differentiation, the downregulation of these genes could be due to negative feedback following protein synthesis of the cytoskeleton at the later timepoints. The expression of specific proteins at certain a time point will be the sum of both synthesis and breakdown of these proteins, and consequently it is impossible from our gene expression data to conclude on protein expression or function of the different timepoints. *Myom2,* another structural gene, peaks at T_5 and T_{10} and shows lesser expression at $T_{15,}$ which supports the notion of early upregulation of structural genes as the cells remodel. Previous studies have reported increased SERCA2 protein and mRNA expression following differentiation of H9c2 cells (8). We did however not find an increase in atpa2a2, which again does not conclude on the protein content of SERCA2.

We also investigated the expression of certain genes as indicators of metabolic remodeling in the H9c2 cells following differentiation. PGC1β, a gene involved in mitochondrial biogenesis, was markedly upregulated and peaked already at T_5 and T_{10}. This supports the existing literature on increased mitochondrial mass with differentiation of the H9c2 cells (12). Our immunostaining of TOM20 on fixed cells also supports the notion of a more extended and dense mitochondrial network following differentiation. The metabolic genes CD36, UCP3 and PDK4, are all involved in metabolism handling of fatty acids. The mRNA expression of these genes are significantly upregulated at all timepoints compared to T_0. Interestingly, the increase in *ucp3*, *pdk4* and *cd36* happens even without any changes in the FA-content in the culturing medium. This favors a metabolic shift towards a more oxidative pheotype due to maturing of the cells, rather than environmental response. PDK4 is a gene involved in regulating metabolism, metabolic switches and in fatty acid handling (31, 32). As this gene

continues to increase its expression at every time point, it is likely that the cells improves its ability to metabolize fatty acids throughout the extended differentiation time. Our culturing media has quite low concentrations of FAs, and as the medium is changed every other day, the concentration of FAs would if anything be reduced by a higher metabolism, again pointing to intrinsic changes within the cells most likely due to a response to RA (33). Increased mRNA expression of PDK4 and fatty acid oxidation with treatment of RA has previously been reported (34), supporting our data on increased on *pdk4* expression.

Uncoupling protein 3 (UCP3) is a natural uncoupler protein associated with the mitochondria. Because it increases its activity with increased fatty acid β oxidation in the mitochondria, an upregulation of this could both be due to the higher mitochondria content together with differentiation and a sign of metabolic shift towards oxidative metabolism. The mitochondria are not only the "power house" of the cell, but also a place for production of reactive oxygen species (ROS). The uncoupler proteins are known to have a role in protecting the cells against harmful ROS-molecules, by lowering the concentration of free electrons that would otherwise react with oxygen to produce superoxide or hydrogenperoxide (16, 35).

We were interested in looking at the mitochondrial function at different timepoints, and performed respirometry to assess changes in cellular oxygen consumption. The respirometry experiments shows a trend for increased oxidative phosphorylation and electron chain capacity in permeabilized cells with longer differentiation protocols, with a peak at T_{10}. When we normalize to cell count, the increase is more evident than with normalization to CS activity. This could be explained by the observed increase in CS activity following longer differentiation. CS activity is an established marker of mitochondrial content, and increased differentiation-induced mitochondrial density has been reported previously in several studies(12). Consequently, an increase in oxidative phosphorylation per cell can be explained largely by the increase in mitochondrial content. Normalization to cell count cannot assess whether the effectivity or respiration rate has increased per mitochondria. Our data shows that by normalizing the data to CS activity, the OXPHOS capacity and the activity of the electron transport chain seem to be stable across the undifferentiated and the differentiated permeabilized cells. Looking at the intact cells, there is no clear increase in cellular respiration following differentiation, neither at basal respiration on the DMEM media, or following addition of Cccp (electron chain capacity). Interestingly, when normalizing for CS activity, the respiratory capacity seems to be lower following differentiation protocols. There is an ongoing discussion about what method one chooses for normalization of the data. Here

we show normalization to “per million cells” and CS activity. The results appear somewhat different with each method for normalizing, which also shows why it is important to be aware of what method one chooses.

The oxygen consumption was markedly down from the undifferentiated cells to differentiated in intact cells at ETC-CI. The exact reason is unknown, but it can be speculated that the non-mitochondrial oxygen-consumption is higher in the undifferentiated cells than the differentiated ones. When calculating the non-mitochondrial respiration at T_0, T_5, T_{10} and T_{15}, it is reduced from 7% at T_0 to 3% in the following time points. The same trends were seen after addition of Antimaycin A, results not included here.

Our data from respirometry with intact cells, shows an increase in the cells’ spare capacity. The increased spare capacity shows an increased tolerance of the cells toward stress or processes demanding a higher ATP-demand. Considering that this is a non-beating cell line, the ATP-demand does not vary as much as in a beating heart. This is rather a response to RA-induced differentiation toward an adult cardiac phenotype.

The differences seen in respiration between the permeabilized cells and intact cells, can be explained by the availability of substrates. The intact cells are dependent on transport proteins for delivery of substrates to feed the oxidative phosphorylation. This is a limiting factor, whereas the permeabilized cells have substrates available in abundance. Additionally, the content of the respiration medium will affect the cells during respiratory experiments.

Collectively, our data from gene expression, respirometry and immunostaining, are indicative of a metabolic and morphologic remodeling induced by treatment with RA and low serum concentration in the culturing medium. This is supportive of already existing literature. In further studies on the cell line, environmental influences like higher FA-content in the culturing medium, are of interest to us.

When doing research on the H9c2 cell line, researchers can choose whether to use undifferentiated or differentiated cells. The advantage to using undifferentiated ones is a shorter protocol and a more homogenous cell population, i.e. these are easier in use than the differentiated cells. Still, one has to consider if this model is relevant in use for the desired purpose. The outcome of a study will vary with the differentiation state of the cells, where the metabolic profile of the mature H9c2 is closer to what is present in an adult cardiomyocyte. The advantage to using differentiated H9cs cells is an oxidative metabolism and a

morphology resembling an adult cardiomyocyte. However, there is a problem that the cell population is non-homogenous. This reduces the applicability of the model, and is probably the reason why many researchers still prefer to use the undifferentiated H9c2 cells. Basal research is important to elucidate molecular mechanisms in health and disease, although there is always a gap between basal research and clinical manifestation of a condition in humans. Therefore, it is important to establish good research models to increase the applicability to in vivo processes.

The use of cell line for research, enables research where systemic factors are eliminated. Researchers have better control of the effect of a treatment, when using a cell line compared to studies performed in humans. Cell-studies are beneficial in use as it is an animal-free alternative way to elucidate molecular and cellular mechanisms in health and disease.

This study has some limitations. Considering that we have 3-4 n in all of our experiment groups, the results can only be regarded as trends at this point. Further experiments are needed to make conclusions about a potential new protocol. Translational experiments conducted in this study, does not always reflect the protein synthesis of the transcribed gene. Specific protein analysis are necessary to gain more knowledge about the functional proteins in the cell line following RA-induced differentiation.

7 References

1. Ambrosy AP, Fonarow GC, Butler J, Chioncel O, Greene SJ, Vaduganathan M, et al. The global health and economic burden of hospitalizations for heart failure: lessons learned from hospitalized heart failure registries. J Am Coll Cardiol. 2014;63(12):1123-33.
2. Zhang XJ, Tan H, Shi ZF, Li N, Jia Y, Hao Z. Growth differentiation factor 11 is involved in isoproterenolinduced heart failure. Mol Med Rep. 2019;19(5):4109-18.
3. Kemp CD, Conte JV. The pathophysiology of heart failure. Cardiovasc Pathol. 2012;21(5):365-71.
4. Luedde M, Spehlmann ME, Frey N. Progress in heart failure treatment in Germany. Clin Res Cardiol. 2018;107(Suppl 2):105-13.
5. Hescheler J, Meyer R, Plant S, Krautwurst D, Rosenthal W, Schultz G. Morphological, biochemical, and electrophysiological characterization of a clonal cell (H9c2) line from rat heart. Circ Res. 1991;69(6):1476-86.
6. Kankeu C, Clarke K, Van Haver D, Gevaert K, Impens F, Dittrich A, et al. Quantitative proteomics and systems analysis of cultured H9C2 cardiomyoblasts during differentiation over time supports a 'function follows form' model of differentiation. Mol Omics. 2018;14(3):181-96.
7. di Giacomo V, Rapino M, Sancilio S, Patruno A, Zara S, Di Pietro R, et al. PKC-delta signalling pathway is involved in H9c2 cells differentiation. Differentiation. 2010;80(4-5):204-12.
8. Branco AF, Pereira SP, Gonzalez S, Gusev O, Rizvanov AA, Oliveira PJ. Gene Expression Profiling of H9c2 Myoblast Differentiation towards a Cardiac-Like Phenotype. PLoS One. 2015;10(6):e0129303.

9. Watkins SJ, Borthwick GM, Arthur HM. The H9C2 cell line and primary neonatal cardiomyocyte cells show similar hypertrophic responses in vitro. In Vitro Cell Dev Biol Anim. 2011;47(2):125-31.
10. Rosano GM, Vitale C. Metabolic Modulation of Cardiac Metabolism in Heart Failure. Card Fail Rev. 2018;4(2):99-103.
11. Pereira SL, Ramalho-Santos J, Branco AF, Sardao VA, Oliveira PJ, Carvalho RA. Metabolic remodeling during H9c2 myoblast differentiation: relevance for in vitro toxicity studies. Cardiovasc Toxicol. 2011;11(2):180-90.
12. Comelli M, Domenis R, Bisetto E, Contin M, Marchini M, Ortolani F, et al. Cardiac differentiation promotes mitochondria development and ameliorates oxidative capacity in H9c2 cardiomyoblasts. Mitochondrion. 2011;11(2):315-26.
13. Tuomainen T, Tavi P. The role of cardiac energy metabolism in cardiac hypertrophy and failure. Exp Cell Res. 2017;360(1):12-8.
14. Doenst T, Nguyen TD, Abel ED. Cardiac metabolism in heart failure: implications beyond ATP production. Circ Res. 2013;113(6):709-24.
15. Nolfi-Donegan D, Braganza A, Shiva S. Mitochondrial electron transport chain: Oxidative phosphorylation, oxidant production, and methods of measurement. Redox Biol. 2020;37:101674.
16. Cadenas S. Mitochondrial uncoupling, ROS generation and cardioprotection. Biochim Biophys Acta Bioenerg. 2018;1859(9):940-50.
17. Perl E, Waxman JS. Reiterative Mechanisms of Retinoic Acid Signaling during Vertebrate Heart Development. J Dev Biol. 2019;7(2).
18. Pagano M, Naviglio S, Spina A, Chiosi E, Castoria G, Romano M, et al. Differentiation of H9c2 cardiomyoblasts: The role of adenylate cyclase system. J Cell Physiol. 2004;198(3):408-16.
19. Menard C, Pupier S, Mornet D, Kitzmann M, Nargeot J, Lory P. Modulation of L-type calcium channel expression during retinoic acid-induced differentiation of H9C2 cardiac cells. J Biol Chem. 1999;274(41):29063-70.
20. Garcia I, Calderon F, la Torre P, Vallier SS, Rodriguez C, Agarwala D, et al. Mitochondrial OPA1 cleavage is reversibly activated by differentiation of H9c2 cardiomyoblasts. Mitochondrion. 2021;57:88-96.
21. Patten V, Chabaesele I, Sishi B, Van Vuuren D. Cardiomyocyte differentiation: Experience and observations from 2 laboratories. SA Heart. 2017;14(2):96-107.
22. D'Amico MA, Ghinassi B, Izzicupo P, Di Ruscio A, Di Baldassarre A. IL-6 Activates PI3K and PKCzeta Signaling and Determines Cardiac Differentiation in Rat Embryonic H9c2 Cells. J Cell Physiol. 2016;231(3):576-86.
23. Kanda T, Takahashi T. Interleukin-6 and cardiovascular diseases. Jpn Heart J. 2004;45(2):183-93.
24. Chacko BK, Kramer PA, Ravi S, Benavides GA, Mitchell T, Dranka BP, et al. The Bioenergetic Health Index: a new concept in mitochondrial translational research. Clin Sci (Lond). 2014;127(6):367-73.
25. Readnower RD, Brainard RE, Hill BG, Jones SP. Standardized bioenergetic profiling of adult mouse cardiomyocytes. Physiol Genomics. 2012;44(24):1208-13.
26. Vandesompele J, De Preter K, Pattyn F, Poppe B, Van Roy N, De Paepe A, et al. Accurate normalization of real-time quantitative RT-PCR data by geometric averaging of multiple internal control genes. Genome Biol. 2002;3(7):RESEARCH0034.
27. Auxerre-Plantie E, Nielsen T, Grunert M, Olejniczak O, Perrot A, Ozcelik C, et al. Identification of MYOM2 as a candidate gene in hypertrophic cardiomyopathy and Tetralogy of Fallot, and its functional evaluation in the Drosophila heart. Dis Model Mech. 2020;13(12).
28. Lange S, Pinotsis N, Agarkova I, Ehler E. The M-band: The underestimated part of the sarcomere. Biochim Biophys Acta Mol Cell Res. 2020;1867(3):118440.
29. Shao D, Liu Y, Liu X, Zhu L, Cui Y, Cui A, et al. PGC-1 beta-regulated mitochondrial biogenesis and function in myotubes is mediated by NRF-1 and ERR alpha. Mitochondrion. 2010;10(5):516-27.

30. Zhao L, Cheng G, Jin R, Afzal MR, Samanta A, Xuan YT, et al. Deletion of Interleukin-6 Attenuates Pressure Overload-Induced Left Ventricular Hypertrophy and Dysfunction. Circ Res. 2016;118(12):1918-29.
31. Pettersen IKN, Tusubira D, Ashrafi H, Dyrstad SE, Hansen L, Liu XZ, et al. Upregulated PDK4 expression is a sensitive marker of increased fatty acid oxidation. Mitochondrion. 2019;49:97-110.
32. Roche TE, Hiromasa Y. Pyruvate dehydrogenase kinase regulatory mechanisms and inhibition in treating diabetes, heart ischemia, and cancer. Cell Mol Life Sci. 2007;64(7-8):830-49.
33. Kuznetsov AV, Javadov S, Sickinger S, Frotschnig S, Grimm M. H9c2 and HL-1 cells demonstrate distinct features of energy metabolism, mitochondrial function and sensitivity to hypoxia-reoxygenation. Biochim Biophys Acta. 2015;1853(2):276-84.
34. Amengual J, Garcia-Carrizo FJ, Arreguin A, Musinovic H, Granados N, Palou A, et al. Retinoic Acid Increases Fatty Acid Oxidation and Irisin Expression in Skeletal Muscle Cells and Impacts Irisin In Vivo. Cell Physiol Biochem. 2018;46(1):187-202.
35. Zhao RZ, Jiang S, Zhang L, Yu ZB. Mitochondrial electron transport chain, ROS generation and uncoupling (Review). Int J Mol Med. 2019;44(1):3-15.

8 Appendix

8.1 Appendix 1: Chemicals

1. **Glucose medium (DMEM)**: Dmem (Glucose medium: D5796, Sigma Life Science) + 10% Fetal Bovine Serum (FBS: F7524, Sigma Life Science) + Strep pen (Penicillin Streptomycin: P0781, Sigma Life Science).
2. **PBS (Dulbecco's Phosphate Buffered Saline)**: D8537, Sigma Life Science
3. **Trypsin**: T3924, Sigma Life Science
4. **MIR05 (Mitochondrial Respiration-medium)**: EGTA (E3889, Sigma Life Science) + MgCl2x6H2O (1.05833.0250, Merck) + Taurine (15,244-2, Aldrich) + KH2PO4 (1.04873, Merck) + HEPES (H7523, Sigma Life Science) + Sucrose (16104, Rieldel) + k-lactobionate (L2398, Sigma Life Science) + BSA, essential fatty acid free (A6003) + Catalase (2000-5000 units/mg protein)(C9322, Sigma Life Science).
5. **Rotenone (Rot)**: R8875, Sigma Life Science
6. **Succinate (Succinate disodium alt, hexahydrate)**: S2378, Sigma Life Science
7. **Digitonin (Dig)**: 37008, Fluka
8. **Adenosine Triphosphate (ADP)**: A5285, Sigma Life Science
9. **Cytochrome C (Cyt C)**: C7752, Sigma Life Science
10. **Oligomycin (Oligo)**: O4876, Sigma Life Science
11. **Antimycin A (Anti A)**: A8674, Sigma Life science
12. **Malate (L-Malic acid)**: M1000, Sigma Life Science
13. **Pyruvate (Pyruvic acid sodium salt)**: P2256, Sigma Life Science
14. **Carnitine (Carn)**: C0283, Sigma Life Science
15. **Palmityl-CoA (PalCoA)**: P9716, Sigma Life Science